



Enhancing Humidity Performance: Effect of Electrode Material on Electrochemical Reduced Graphene Oxide (ERGO) Humidity Sensor

Norhazlin Khairudin¹, Mohammad Haziq Ilias¹, Rozina Abdul Rani²
Muhammad Zamharir Ahmad³, Azrif Manut¹, Norhafizah Burham¹, Majid
Nour⁴, Ahmad Sabirin Zoolfakar^{1*}

¹School of Electrical Engineering, College of Engineering,
Universiti Teknologi MARA, Shah Alam, 40450, MALAYSIA

²School of Mechanical Engineering, College of Engineering,
Universiti Teknologi MARA, Shah Alam, 40450, MALAYSIA

³Biotechnology & Nanotechnology Research Centre, Malaysian Agricultural Research & Development Institute,
MARDI Headquarters, Serdang, 43400, MALAYSIA

⁴Electrical and Computer Engineering Department,
King Abdulaziz University Jeddah, SAUDI ARABIA

*Corresponding Author

DOI: <https://doi.org/10.30880/ijie.2022.14.03.024>

Received 14 December 2021; Accepted 07 June 2022; Available online 20 June 2022

Abstract: Reduced graphene oxide (rGO) possesses remnant oxygen functional groups, hydrophilic characteristics, and a large surface area, making it a one-of-a-kind material with unique qualities that are attributed to the reduction of graphene oxide (GO) process. There are numerous ways that can be utilized in the reduction process; however, it has not yet been completely examined which method is the most efficient in terms of reducing the oxygen-containing functional group from the GO. This is owing to the fact that a successful reduction technique has the potential to broaden the scope of rGO's applicability across a wide range of industrial sectors. This study entails an investigation the effect of humidity performance on different metal materials such as Pt, Au, Ag, and Cu with fixed fingers spacing of 5µm on the reduced graphene oxide (rGO) by electrochemical deposition (ECD) from GO aqueous dispersion. A combination of experimental measurements using humidity chamber, Raman spectroscopy, Electrochemical Impedance Spectroscopy, and Scanning Electron Microscopy have revealed the performance of rGO as the humidity sensor. According to the findings, a good humidity performance was displayed in rGO/Pt, as demonstrated by higher sensitivity and greater response towards humidity which is found to be around 10 times higher response than GO in Hummer's method, as reported in the literature. These characteristics are both facilitated by the higher ionic conductivity of the material.

Keywords: Electrochemically Reduced Graphene Oxide (ErGO), Electrochemical deposition (ECD), Electrochemical Impedance Spectroscopy (EIS), humidity characterization, electrochemical behaviour

1. Introduction

Sensors for humidity are widely employed in a range of industries, including healthcare [1], industrial processing, agricultural monitoring [2], domestic machine controlling [3], food processing, and environmental monitoring [4]. They continuously monitor, detect, and adjust the ambient humidity under a variety of situations, from low to high temperatures and in combinations with other gases. Regulation of humidity is critical for human health and comfort, as well as the quality of products in the food, environment, chemical, and semiconductor industries [5]. As a result, the importance of accurate, precise, and effective humidity monitoring has increased in recent years. Ideal humidity sensors should meet a number of specific characteristics, including high sensitivity, speed of response/ recovery times, physical stability, reproducibility and the capacity to operate across a wide temperature range [6]. Sensor dependability can be influenced by a variety of elements, including the morphology of the structure as a surface reaction, the substrate used as the sensing medium, and the preparation method. Therefore, there are numerous materials have been researched as a promising medium for humidity sensors, including metal oxides [7], spinel compound [8], perovskite compounds, [9] semiconductors [2], polymers [10], carbon-based material [11] and ceramics [12] [13] [14]. Among these, researchers are focusing their attention on carbon-based materials such as graphene, graphene oxide and reduced graphene oxide, carbon porous materials and carbon nanotubes for humidity sensing applications recently and the corresponding research has lasted more than a century [15]. Humidity sensors display the degree of humidity in an environment by converting the amount of water molecules in the environment into a signal. This is based on the changes in physical properties that occur when water molecules interact with a material [9].

Two-dimensional carbon nanomaterial graphene sp^2 has gained substantial attention due to its excellent physicochemical, electrical, optical, thermal, mechanical, and biocompatibility properties as well as its ability to conduct electricity. Its unique atomic arrangement facilitates the use of graphene materials in electronics, energy generation and storage, optoelectronics, catalysis, and chemical sensors, among other fields of application. Graphene is a single sheet of graphite with a zero-band gap, in contrast to graphite's metallic feature. Graphene is a promising material for future applications. While operating at low temperatures, the carrier density can reach up to 10^{13}cm^{-2} , and the carrier mobility can reach $10,000 \text{ cm}^2 \text{V}^{-1} \text{s}^{-1}$ [16] at high room temperature and $200,000 \text{ cm}^2 \text{V}^{-1} \text{s}^{-1}$ [17][18]. Graphene's Young's modulus is 1.1TPa [16], which is greater than the tensile strength of steel. Because of its excellent mechanical properties, which are the result of its perfectly ordered atomic arrangement, graphene is an ideal material for stretchable and wearable electronic devices, such as smart watches. The exceptional transparency of this material, as well as its low sheet resistance of approximately $30 \Omega \text{ sq}^{-1}$, are crucial characteristics of this material, which has great potential for high-performance optical and electrical devices. Due to its exceptionally high specific surface areas, graphene can have a specific surface area of up to $2600 \text{m}^2/\text{g}$ [19], and as a result, it has demonstrated substantial aptitude for gas detection in a wide range of conditions [20] [21].

The aforementioned features are only exhibited in pristine graphene qualities, in contrast to graphene derivatives produced by the solution approach instance GO and rGO. The approach primarily introduces the oxygen functional groups such as hydroxyl (-OH), epoxide (-O-), carboxyl (-COOH) and also imperfection structure on the basal plane of graphene derivatives [17][22]. As a result, the GO transforms into an insulator that lacks conductivity, necessitating the reduction procedure in order to be functional in the vast majority of real-world applications. More importantly, structural flaws, functional oxygen groups, and other impurities reduce physical qualities of rGO including as mechanical properties, conductivity, and transparency, as reported in [23]. Nonetheless, when exposed to groups with high oxygen concentrations in aqueous solutions, these graphene derivatives exhibit a variety of responsive behavioral stimuli, which can be chemically modified to improve their properties and make them more useful for other applications, as described in [24]. Meanwhile, the electronic characteristics of rGO can be altered by using doping and functional group joining, respectively, to acquire additional qualities [25][26]. It's also possible to produce a variety of graphene-based composite structures by using non-covalent interactions between graphene or rGO and other components and also can dispersed in solution made into 3D porous structures, films, and fibers that can be used in a wide range of applications [27][28]. According to [25][2][29], rGO-based humidity sensors have lower sensitivity than GO-based sensors due to the lower functional oxygen-containing group in the sensors. However, combining the rGO with other sensitive materials can further increase the sensitivity of the sensor. Therefore, in order to strengthen and expand the performance of humidity sensors, based on rGO materials, more research and development is required to be carried out in the future. In addition, the internal electric field created in the heterojunction makes it easier to separate photogenerated charge carriers and regulate electron transport, hence heterostructure materials have been extensively studied to date in a variety of device applications. Van De Wall's force can thus be used to generate the p-n heterojunction, leading to the transfer of electrons between the interface and enhancing the humidity sensing capability of rGO material in contact with a metal electrode [3][6][30].

Here, we demonstrated a humidity sensor based on electrochemically reduced graphene oxide (ErGO) film synthesized via electrochemically reduction process which the layers of thin film rGO are deposited onto the different electrode materials, including Aurum (Au), Platinum (Pt), Silver (Ag), and Copper (Cu), with $5 \mu\text{m}$ of finger spacing. The cyclic voltammetry (CV) window parameters are set identically for all the samples in water bath at temperature 40°C . The humidity performance and electrochemical reaction were investigated. The material dependent humidity response of rGO based on ionic conductivity produced when the water molecules absorption on the surface of rGO and produce

numbers of hydronium ion resulting the proton and charge transfer occurrences. The device performance has been studied based on calculated humidity measurement on resistance, response, sensitivity, stability, reproducibility, response time as well as recovery time. The results depicted the humidity performance; the humidity working in negative resistive mode as the resistance is inversely proportional with varying humidity level. The linear correlation between sensitivity and responsivity toward humidity was recorded on the fabricated samples. The response time was examined via the speed of absorption water molecules thru the rGO-metal interface and recovery time indicate the desorption of water molecules from the multilayer interface to reach the equilibrium similar to external humidity level. The humidity sensor exhibited higher sensitivity and higher responsivity over the wide range of humidity level fall on the rGO/Pt.

2. Material and Methods

2.1 Preparation of Graphene Oxide (GO) Solution

A beaker was filled with a PH 7.4 PBS solution (R&M Chemicals). Continuously apply sodium hydroxide granules (Sigma, Aldrich) until PH 9 was attained. After that, 0.15g graphite powder (C, Aldrich 99%) was used to agitate the PBS solution magnetically for 15 minutes.

2.2 Fabrication of Reduced Graphene Oxide (Rgo) Via Electrochemical Deposition (ECD)

Fig.1 (a)-(b) depicts the experimental setup. The electrochemical procedure for rGO deposition was carried out utilizing three common electrodes: working electrode (WE), counter electrode (CE), and reference electrode (RE). These electrodes were assigned to three separate probes that are attached to the electrochemical deposition (ECD) system machine. The 50 ml GO solution was poured into the glass container. All electrodes are placed in glass container containing GO solution. After that, the glass container was immersed in a 40°C deionized water bath and left for a few minutes to attain equilibrium temperature. Following that, a cyclic voltammetry (CV) analysis was performed. The voltammetry window parameters utilized were -0.4V to -1.1V sweep potential (lower and upper vertex), 10 scan cycles, and 0.005 V/s scan rate. Each window parameter was assessed at -0.2V (start-stop potential) on an interdigital electrode comprised of Au, Cu, Pt, and Ag. On the conducting electrode surface, rGO thin films were deposited by the electrochemical deposition (ECD) method. The final morphology/structure of ErGO films is significantly influenced by CV parameters, electrolyte properties (recipe and temperature), electrodeposition time, and applied potentials. After the deposition is completed, the sample was dried at room temperature.

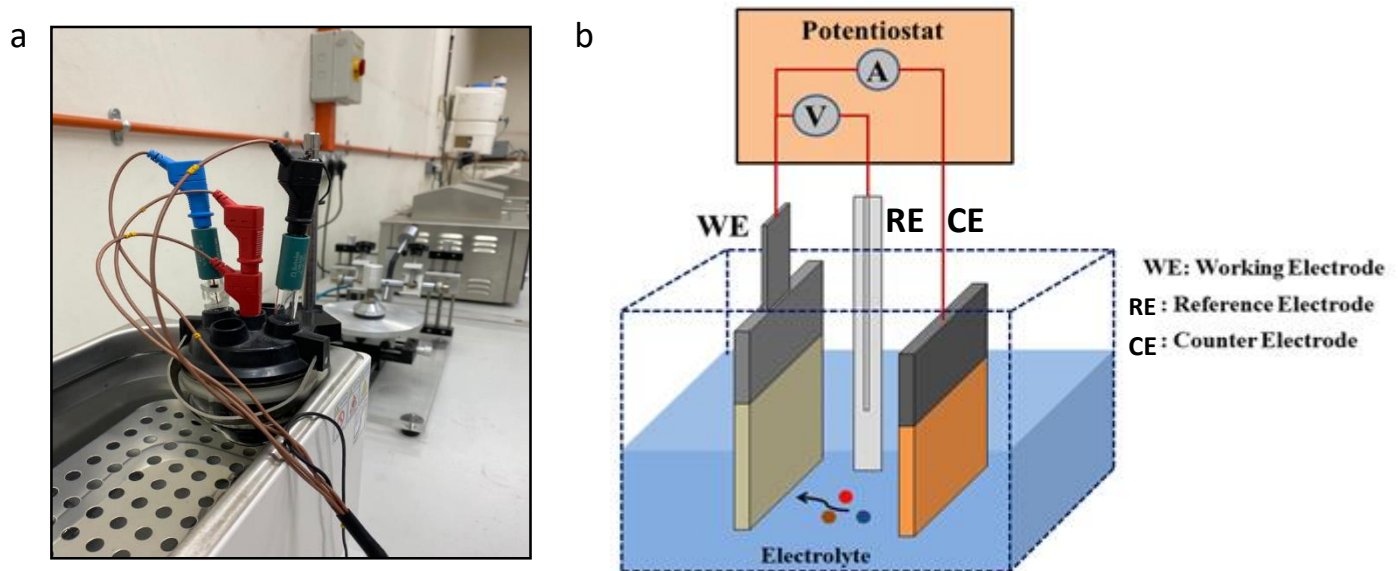


Fig. 1- (a) The arrangement for electrochemical deposition (ECD) process; (b) the schematic diagram of electrodeposition technique

2.3 Material Characterization

The rGO thin layer produced on the metal electrode surface was investigated using Raman spectroscopy. A 514nm laser was used to stimulate the samples in Raman spectroscopy. The molecular vibration or structural information of fabricated samples was investigated. The characteristic peaks of reduced graphene oxide's Raman spectra are denoted by D (disorder) and G (graphitic). In contrast, scanning electron microscopy (SEM) was employed to analyze the surface morphology of the sensing layer of the samples, with a SEM machine operating at an accelerating voltage 5kV.

2.4 Humidity Response Properties and Electrochemical Characterization

The performance of the fabricated samples can be evaluated by measuring the electrochemical system's impedance throughout a specified frequency range. This analysis fits current, voltage, and frequency data to the equivalent circuit (EC) model. Resistance models depict cell solution (R_s), constant phase element (CPE), and charge transfer resistance (R_p). The FRA window parameter was set to a frequency range of 10Hz to 1Mhz and 0.2V of applied potential. The internal resistances and impedances were developed by fitting examination. The sensor performance was evaluated via a humidity chamber (ESPEC SH261) with sensor measurement (Keithley 2400). To produce I-t curve findings, the samples were electrically tested for 40%RH to 90%RH, 5 cycles at 25°C, 0.2V applied voltage, and 100,000 measurement points. 2 (a) illustrates the arrangement of apparatus for electrochemical impedance spectroscopy measurement using an AUTOLAB PGSTAT101 equipped with NOVA software, whereas Fig. 2 (b) depicts the arrangement for humidity test measurement.

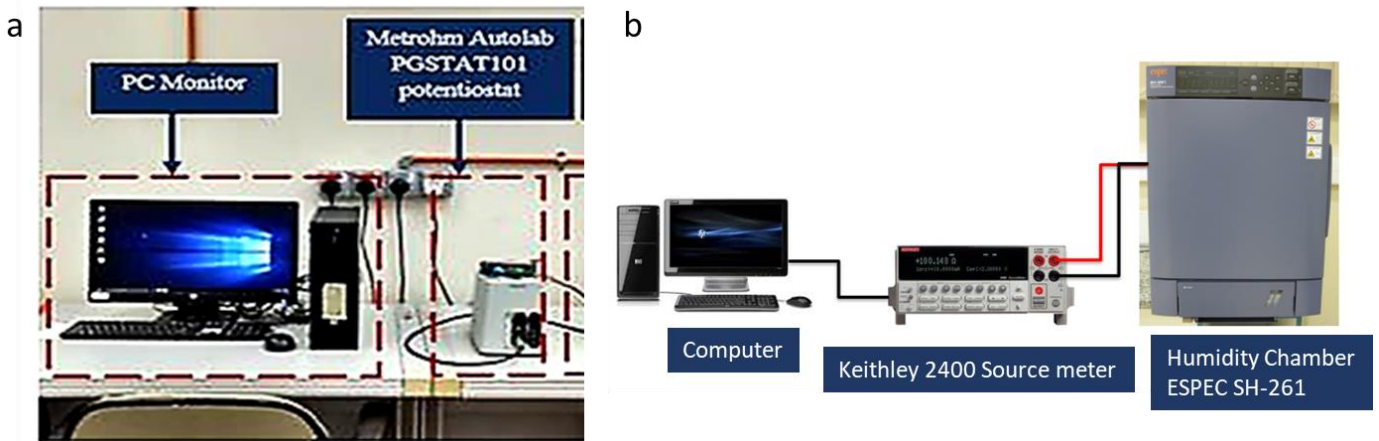


Fig. 2 - (a) The arrangement for electrochemical measurement; (b) the apparatus set up for humidity measurement

The performance of humidity sensing was evaluated through the importance parameter such as their sensitivity, speed response time/recovery time, reproducibility and stability.

Sensitivity

A resistive humidity sensor works on the idea that water molecules adsorb on the humidity-sensitive film, altering the film's impedance properties. By altering the output electrical signal, these sensors determine the ambient humidity. A resistive humidity sensor's sensitivity can be calculated by equation (1) follows:

$$S = \frac{Ra}{Rrh} \quad (1)$$

In this equation, S denotes the sensitivity, Ra refers the resistance of the sensor while exposed to the beginning humidity level, and Rrh indicates the resistance of the sensor when exposed to the specific humidity level

Response time and Recovery time

Response time is defined as the time period required for the response to increase from 10% to 90% of its highest value. The rise time derived from the I-t curve can be estimated with the aid of equation (2). On the other hand, recovery time, is the time interval required for the response to decline from 90 % of its peak value to 10 % of its peak value, it can be estimated using equation (3).

$$\tau_r = t_{10} - t_{90} \quad (2)$$

$$\tau_f = t_{90} - t_{10} \quad (3)$$

Reproducibility

Reproducibility is the ability of a transducer's sensor to duplicate output measurements when applied with the same voltage potential value, circumstances, and direction.

Stability

The stable sample is one in which the current drops only a little amount, indicating stable operation. It indicated the current that had been produced consistently over a period of time.

3. Results and Discussions

3.1 Characterization of Rgo Film

Raman spectroscopy was utilized to investigate structural morphology changes during electrochemical GO reduction. Fig. 3 depicted, the rGO spectrums had two strong notable Raman-active peaks at 1359cm^{-1} and 1607cm^{-1} allocated to the D and G-bands in the rGO spectrums, respectively. The D band represents rGO defects, while the G band represents the sp^2 carbon pair in network. Thus, the intensity ratio of the D and G bands of rGO ($I_D/I_G=0.85$), which indicates that hydroxyl, epoxy, and carboxyl of oxygen functional groups have been reduced from reduction process from GO to rGO via electrochemically deposition. Due to this process, it induced the defect in the structure as described in [31][29][32].

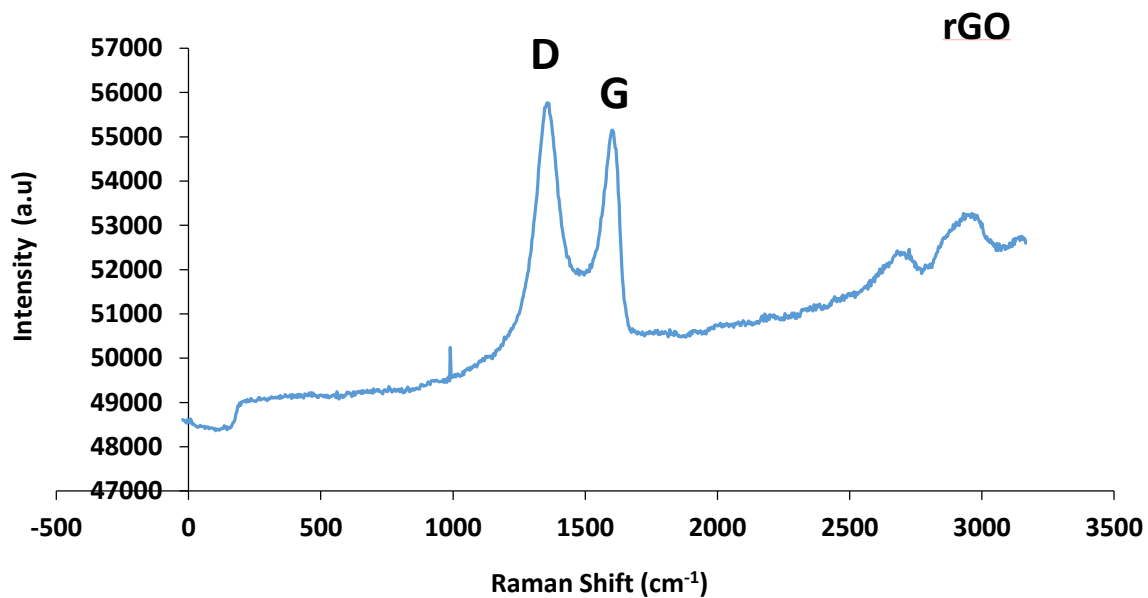


Fig. 3 - Raman spectra of the rGO

3.1.1 Scanning Electron Microscope (SEM)

Fig.4-(a)-(d) illustrated the surface morphology of the rGO is distributed on the surface of substrate was performed using the Scanning Electron Microscope (SEM). The rGO possess creased, wrinkled and ripple structure caused by the reduction deformation of GO to rGO thus showing an increase in the specific surface area of the rGO/metal. The higher specific surface area on the substrate facilitates the absorption of water molecules on the rGO surface.

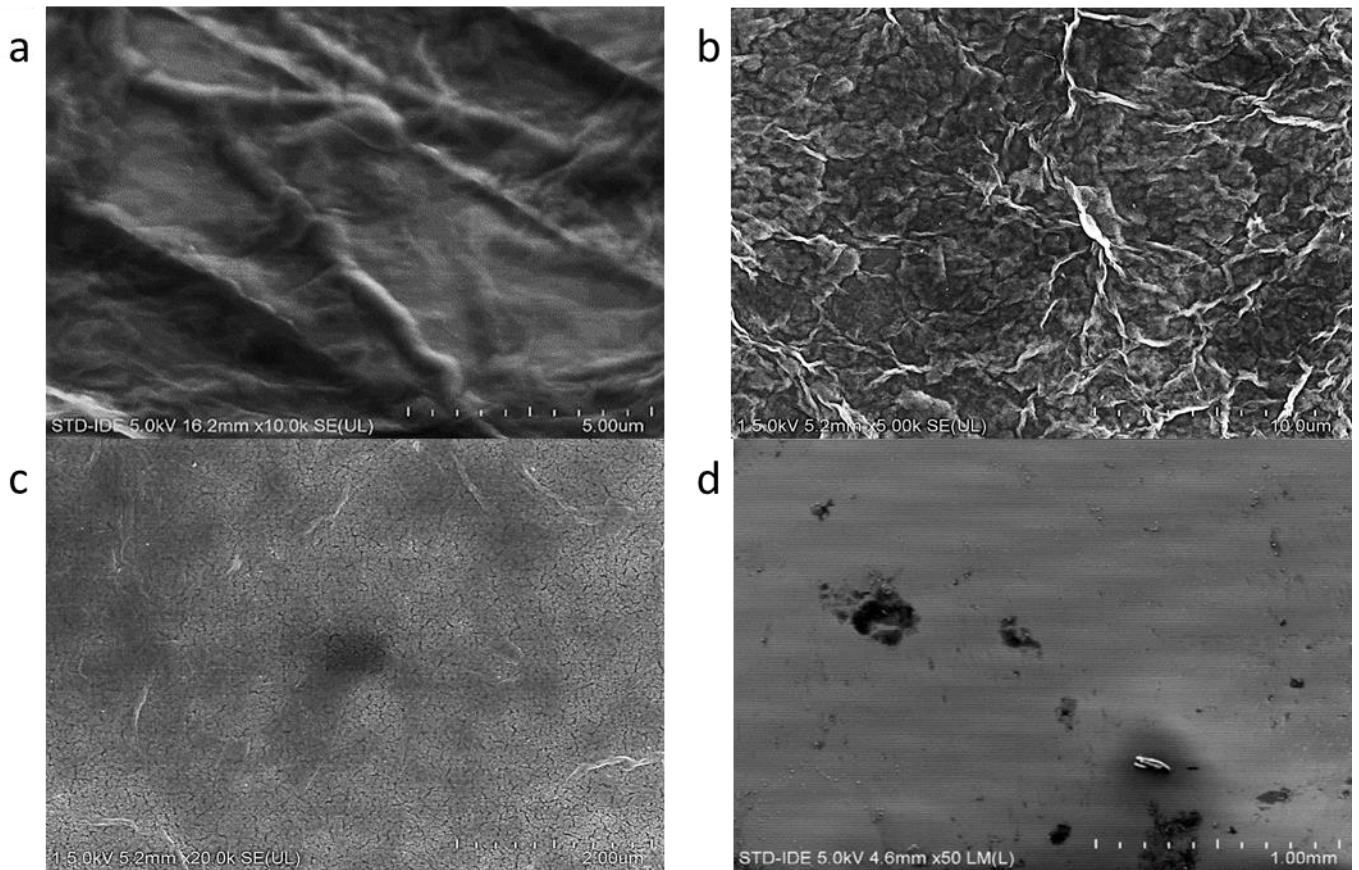
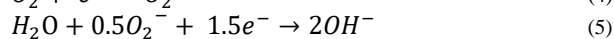


Fig. 4 - FESEM micrographs of (a) 5kV, 5um ErGO; (b) 5kV, 10um ErGO; (c) 5kV, 200um ErGO; (d) 5kV,1mm ErGO

3.2 Humidity Sensing Properties

3.2.1 Humidity Sensing Mechanism

Reduced graphene oxide (rGO) has oxygen-containing groups in the structural layer such as hydroxyl, epoxy, and carbonyl that adsorbs water molecules. A gradual increase in humidity causes the rGO material to agglomerate with water molecules via the interaction between water molecules and the rGO material [12]. These graphene derivatives' hydrophilic characteristics facilitate the absorption of water molecules in their surroundings. As a result, the structural changes in rGO make it appropriate as a sensitive material for humidity sensors [33]. When rGO absorbs oxygen from its surroundings, oxygen ionization occurs, resulting in the creation of superoxide (O_2^-) [15]. This superoxide (O_2^-) production traps valence electrons as well. The ionization process can be described as equation (4) follows:



The presence of superoxide (O_2^-) is significant in the dissociation of water molecules. When rGO begins to be exposed to humidity, superoxide molecules form on the surface of the rGO as a result of the dissociation of water molecules which is equation (5) depicted the dissociation phenomenon [34].

Following that, electrons are transferred to the rGO conduction band as a result of water molecule dissociation. The hydroxide (OH⁻) is formed on the surface of rGO as a result in formation of combination the hydrogen and oxygen bonds. The chemisorbed layer OH⁻ generated on the surface of rGO refers to the hydroxyl layer [29][2][5]. This creation of hydroxyl layer is summarized in equation (6).

When the humidity level changes, the oxygen-containing group forms hydrogen bonds on the inner layer and surface of rGO via the water absorption mechanism. These alterations will have an effect on the hydrogen bonds' intrinsic strength.

At low humidity, water molecules begin to adsorb on the first layer of rGO as illustrated in Fig. 5 (a). The absorption of water molecules is through double hydrogen bonds on the layer. In a double hydrogen bond, water molecules cannot move freely. At this time, proton transfer between neighbouring hydroxyl groups which requires significant amounts of energy, hence rGO has a high resistance. In other words, in response to the interaction between the water molecule and the rGO, the water molecule is drawn to the surface of the rGO where it functions as an electron donor, providing electrons to it and thereby raising the electron density. As a result of the occurrence of annihilation, the number of hole concentrations in the p-type rGO may decrease as a result of recombination process. A consequent rise in rGO resistance is observed. This is owing to the fact that layer expansion arises as a result an increase in the distance between molecules as indicated in [15][31][29].

As the humidity progressively rises, several layers of water molecules accumulate on the surface of the rGO. A single hydrogen bond allows water molecules to be physically absorbed through hydroxyl in the subsequent layer as demonstrated in Fig 5 (b). The mobility of water molecules, as well as exhibiting liquid water, is freely flow in a single hydrogen bond. Thus, many charge carriers are created from ionized water molecules (H₃O⁺) during the absorption of water molecules on multiple layers under the influence of electrostatic fields [35] as depicted in Fig 5 (c). Furthermore, charge and proton transfer occur at the rGO, resulting in a reduction in resistance. From the perspective of the Grotthuss chain reaction can be deduced as equations (7) and (8) below:

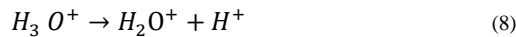


Fig.5 (a)-(c) represented the adsorption of water molecules at different humidity levels onto various physical chemisorbed layers of the deposited rGO material.

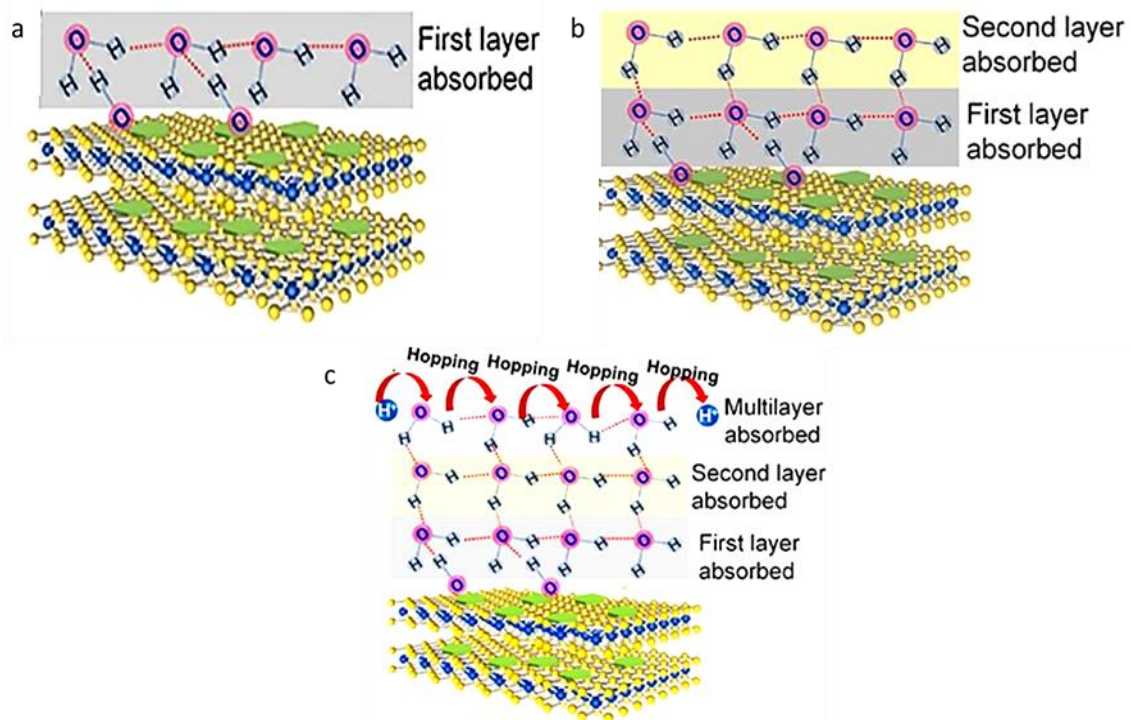


Fig. 5 - (a) Water molecules absorbed in the first layer on the surface of rGO at low humidity; (b) water molecules from the second layer absorbed by the first layer; (c) absorption of multilayer water molecules at high relative humidity. Reproduced with permission from [29] Sensors Actuators, B Chem. Elsevier Copyright, (2021)

3.2.2 Humidity Sensing Performance

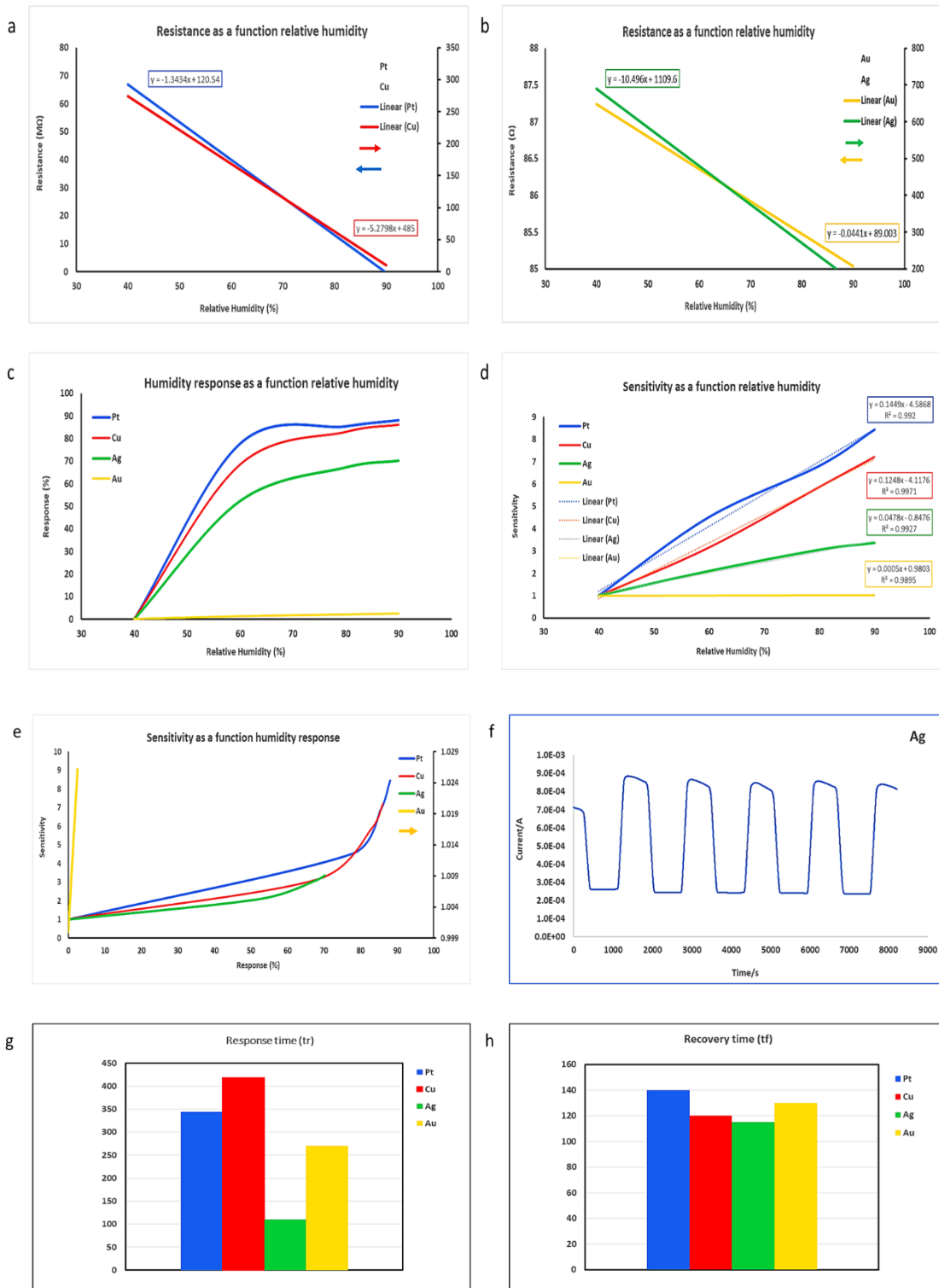


Fig. 6 - Experimental results

Figure 6 experimental results (a) Resistance of rGO changes under different humidity levels from 40% RH-90%RH on Pt and Cu electrode material. (b) Resistance of rGO changes under different humidity levels from 40% RH-90%RH on Ag and Au electrode material. (c) The humidity response of rGO changes under different relative humidity from 40%RH-90%RH on Pt, Cu, Ag and Au electrode material. (d) The sensitivity of rGO on Pt, Cu, Ag and Au material towards different relative humidity. (e) The sensitivity of rGO on Pt, Cu, Ag and Au material towards humidity response.

- (f) The reproducibility of the sensor over the 5 cycles. (g) The response time of rGO on the Pt, Cu, Ag and Au material.
- (h) The recovery time of rGO on the Pt, Cu, Ag and Au material.

The performance of sensor was evaluated based on their sensitivity, response time, recovery time as well as reproducibility. The changes in resistance can be used to assess changes in the humidity, as well as to identify variations in the current. The sensor measures the humidity level in the surrounding environment by translating the measured value into an electrical signal [6]. This is due to the fact that variations in the resistance on the surface of the material for the sensing mechanism can be used to determine the absorption of water molecule concentrations. As demonstrated in this study, rGO demonstrated working in a resistive mode humidity sensor. In terms of equations (9), the resistive humidity response can be represented as follows:

$$Response = \frac{R_h - R_a}{R_a} \times 100\% \tag{9}$$

It is mentioned that R_h represents the resistance that is exposed to the specified humidity level and R_a represents the resistance that is exposed to the beginning humidity level. Using the tabulated data, Fig.6 (a) and (b) exhibited the resistance changes over the range of 40% RH to 90% RH with a fixed 5um spacing distance and a 0.2V applied potential at 25°C throughout the process. The results indicated that a linear regression fit was plotted to determine the inversely linear relationship between resistance and humidity levels. As the relative humidity increases gradually, a multilayer of water molecules forms on the rGO film's surface. Physical adsorption begins in the second layer, as water molecules can freely move in a single hydrogen bond on the hydroxyl, simulating liquid water's behavior. The event may result in the ionization of water molecules and the formation of a significant number of charge carriers H_3O^+ on the rGO surface, where proton and charge transfer occurred, resulting in a decrease in rGO resistance which agreement in line described in [29][34][5].

Whereas, Fig.6 (c) demonstrated the characteristic response of rGO deposited on different metals including Pt, Cu, Ag and Au, to a wide range humidity concentration. The graph depicted a constantly proportional relationship between response and relative humidity (RH) that becomes gradually increased slowly as it approaches towards the end. The curve obtained illustrated the response of rGO deposited on Pt>Cu>Ag>Au at 88.14%, 86.1%, 70.23% and 2.55% correspondingly. The findings demonstrated rGO/Pt has the greater response to humidity when compared to other metal materials (Cu, Ag, and Au), and its response to humidity is approximately 10 times and 3 times higher than that of GO in Hummer's technique and PDDGA/rGO in chemical reduction LbL nano self-assembly fabrication method, respectively as reported in Table 1. The humidity detecting features of the constructed sensor were compared to those of previously published resistive-type graphene-based humidity sensors in Table 1. As can be seen, the proposed sensor's response is equivalent to that of existing resistive-based humidity sensors. Additionally, the suggested sensor has a greater response than all previous published humidity sensors except for [40]. As a result, rGO/Pt appeared to be an attractive material for the fabrication of a high-performance humidity sensor.

Table 1- Humidity sensor performance of this work compared with the literatures

<i>Sensing material</i>	<i>Fabrication method</i>	<i>Measured RH% range</i>	<i>Response (%)</i>	<i>Ref.</i>
rGO/Pt	ECD	40-90	88.14	This work
GO	Hummer	30-95	7.9	[39]
PDDA/rGO	Chemical Reduction	11-97	8.7-37.4	[36]
PRGO-4h	Hydrothermal reduction	20-85	3.3-105	[40]
rGO/PU	Liquid Phase Blending	10-70	2.9	[41]

The graphs in Fig. 6(c), 6(d) and 6(e) are closely interrelated explaining the response-sensitivity relationship in which Fig. 6(d) states that rGO/Pt exhibited higher sensitivity capability of 8.44 towards humidity compared to rGO/Cu, rGO/Ag and rGO/Au, which were 7.1, 3.36 and 1.03 respectively This may be explained by the fact that the sensor's sensitivity is related to its humidity response, as seen in Fig 6(e). According to the acquired data, the rGO/Pt sample had the greatest sensitivity, showing a stronger responsiveness to humidity. This great sensitivity is due to the fact that the rGO films contain a high surface-to-volume ratio, a dense network of surface voids, and a hydrophilic functional group that readily interacts with the surrounding water molecules. Under low humidity conditions, p-type rGO semiconductors produce a positive charge carrier as a result of water molecules absorbing electron donors on the surface of the rGO [15]. Water molecules' chemical absorption reduces the concentration of holes in p-type rGO, resulting in a high resistance of the rGO film. When the humidity is increased gradually, multi-layer adsorbed water molecules develop on the surface of the rGO/Pt film. This results in the formation of a large number of hydronium ion (H_3O^+) charge carriers on the surface of the rGO, where they act as a substantial medium for ionic conductivity across the rGO/Pt film's large interfacial area. Additionally, another sensing mechanism is explained by the defect structure created on the sp³ carbon network when adsorbed water molecules penetrate the multilayer film, resulting in an interlayer expansion effect. The distance between expansion layers modifies the network's connectivity as well increase sensor resistance [9][12][37]. As a result, a trade-off emerges in the humidity sensor between ionic conduction and the interlayer expansion effect.

At high humidity, this system exhibits a decrease in sensor resistance, which can be ascribed to the significantly greater contribution of ionic conductivity compared to the interlayer expansion effect films. According to the preceding description [29], the major sensing mechanism is attributed to the p-type semiconductor properties of rGO at low humidity and the increased ionic conductivity at high humidity.

Fig. 6(f) illustrated the reproducibility and stability of consecutive rGO/Ag films over five consecutively cycles with an interval of 800s at a temperature of 25°C. The graph indicates that minimal current deviation in the rGO/Ag sensor occurs throughout the water molecular absorption and desorption process. The minor variance affirmed the rGO/Ag film's excellent stability and reproducibility in comparison to other metals used, such as Pt, Au, and Cu.

Fig 6(g) and 6(h) illustrated the time-dependent response and recovery. It can be seen that the faster response time is at rGO/Ag > rGO/Au > rGO/Pt > rGO/Cu, which were 110s, 270s, 344s and 418s respectively and the faster recovery time is at rGO/Ag > rGO/Cu > rGO/Au > rGO/Pt were 115s, 120s, 130s and 140s indicating that the rGO/Ag film has the shorter response time and faster recovery time toward the adsorption and desorption process. The absorption of water molecules via the rGO/Ag surface occurs at a faster rate due to the hydrophilic property of rGO, which enables the film to easily trap water molecules in the environment. Additionally, faster response times were observed when hydronium ions (H₃O⁺) were chemically absorbed into the rGO/Ag surface layer. Whereas the rGO/Ag desorption process likewise occurred swiftly in terms of releasing water molecules from the interlayer and achieving equilibrium between the internal water content and the external humidity level. Thus, the sensor's rapid recovery may be demonstrated in the rGO/Ag film which this agreement in line as described in [6][15][38].

3.3 Electrochemical Properties Characterization

Electrochemical impedance spectroscopy (EIS) determines the electrical impedance of a substance as a function of the frequency of an applied electrical current. This enables the electrochemical systems to be characterized using an electrical circuit equivalent (EC) model [42]. EIS presents the collected data in the form of a fitted Nyquist plot, equivalent circuit model. During an electrochemical process, the equivalent circuit represents each component at the interface and in the solution. The models illustrate the resistance of the solution (R_s), the charge transfer resistance (R_p), and the constant phase element (CPE) [43]. The FRA window parameter was selected using a frequency range of 10Hz to 1MHz and a 0.2V applied potential. The impedances and internal resistance were calculated as a result of the fitting evaluation as discovered in Table 2.

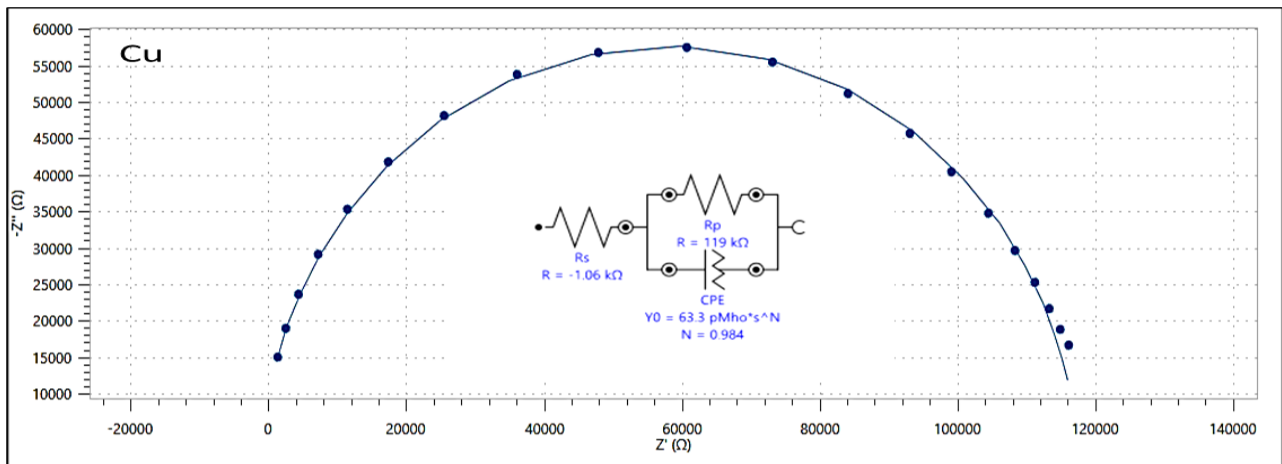


Fig.7 - The Nyquist plot for rGO/Cu at 5um electrode. The graph represented the Z' (Ω) vs Z'' (Ω) at applied potential 0.2V

Fig. 7 represented the Nyquist plot with inset an equivalent circuit (EC) model illustrated the resistance and impedance of the rGO/Cu film. The corresponding graph depicted the semicircle diameter provides the estimation of charge transfer resistance (R_p) at the rGO-metal interface. The interpretation indicates that the arc of the semicircle and the charge transfer resistance are linearly related. The charge transfer resistance (R_p) increases as the radius of the semicircle arc increases. The smaller semicircle arc, the lower the charge transfer resistance at the rGO-metal interface [44][45].

Table 2 - The significant parameters for EIS measurement at applied potential 0.2V

<i>IDE electrode material</i>	<i>Solution Resistance (R_s)/(Ω)</i>	<i>Charge transfer Resistance (R_p)/(Ω)</i>	<i>Constant Phase Element (CPE)</i>	<i>X²</i>
Ag	226.6	862.56	5.697μ	0.0001447
Au	70.6	14.09	60.42μ	0.0017199
Cu	1.06k	118k	63.29p	0.0086063
Pt	109	1.68k	4.201μ	0.0018592

The EIS measurement parameter was calculated from the tabulated Table 2 in order to evaluate the interaction and charge transfer at the rGO-metal interface composites by modelling an equivalent circuit as seen in Fig 7. In the equivalent circuit (EC), the solution resistance (R_s), charge transfer resistance (R_p), and constant phase element (CPE) were all represented. It is discovered that, the charge transfer resistance (R_p) found to be the lower on rGO/Au < rGO/Ag < rGO/Pt and rGO/Cu indicating the smaller radius semicircle arc and a faster charge transfer over the rGO-Au interface. This behaviour is attributed to the fact that rGO/Au has the highest conductivity of all materials tested, which is consistent with the findings in [42][46]. These data imply that when the electrical conductivity increases, the number of electrons that can travel across the rGO-Au contact increases due to the lowered charge transfer resistance barrier (R_p). For example, rGO/Cu has a significantly larger charge transfer resistance of 118k compared to 1.68k, 862.56, and 14.09 for Pt, Ag, and Au. This shows that fewer electrons may pass via the rGO/Cu contact, implying a low contribution of electrical conductivity and a deficient charge transport mechanism. Additionally, the difference in work function between rGO and Au creates a potential barrier between the two materials, allowing electrons to flow across the sensing material and from the lower work function material to the higher work function material. As a result of attaining equilibrium, a new Fermi energy level is formed. Due to the fact that Au's work function (5.1eV) [47] is higher than that of rGO's (4.6eV) [29], electrons pass from rGO's conduction band to Au through band bending, thereby blocking the electron transport channel. Additionally, the number of electrons in Au grows, resulting in the material's high electrical conductivity, as reported in [48][10][5]. As a result, electrons exposed to the sensitive material's surface behave as active sites, increasing the material's electrical conductivity [49]. Since a result, EIS humidity has no direct relationship with humidity performance, as the current generation of humidity characteristics is created by ionic conductivity induced by the creation of high hydronium ions, as well as the generation of protons and charges.

4. Conclusion

In conclusion, this work reported a facile, ecologically friendly, and cost-effective approach for fabricating rGO on a range of noble metals, including Au, Pt, Ag, and Cu for use as a humidity sensor via electrodeposition methods. Raman spectroscopy was used to determine the appearance of the D and G bands in relation to the carbon structure and to establish that the GO had been reduced to rGO throughout the reduction process. The wrinkled structural layer of rGO is detected using a scanning electron microscope (SEM), and the presence of irregular nanosheet waves or ripples suggests that they are caused by the substrate deposition process. Additionally, utilising humidity characteristics and electrochemical impedance spectroscopy, the influence of electrode material on the performance of a humidity sensor was investigated. In this research, the p-type rGO semiconductor was used as a negative resistive humidity sensor. The findings revealed that the rGO/Pt had good humidity performance, as evidenced by its tenfold increased responsiveness to humidity when compared to the GO Hummer's approach stated in the literature. This is because the high concentration of hydronium on the surface of rGO/Pt leads to a significant number of protons hopping between neighbouring water molecules, enhancing the ionic conductivity of rGO/Pt relative to Cu, Ag, and Au.

Acknowledgement

This work is supported by Universiti Teknologi MARA under internal grant known as Geran Penyelidikan Khas (GPK) 600-RMC/GPK 5/3 (089/2020).

References

- [1] Abid, P. Sehrawat, S. S. Islam, P. Mishra, and S. Ahmad, "Reduced graphene oxide (rGO) based wideband optical sensor and the role of Temperature, Defect States and Quantum Efficiency," *Sci. Rep.*, vol. 8, no. 1, pp. 1–13, 2018, doi: 10.1038/s41598-018-21686-2.
- [2] R. Liang, A. Luo, Z. Zhang, Z. Li, C. Han, and W. Wu, "Research progress of graphene-based flexible humidity sensor," *Sensors (Switzerland)*, vol. 20, no. 19, pp. 1–17, 2020, doi: 10.3390/s20195601.
- [3] P. V Shinde and M. Saxena, "Dimensional Heterostructures for Sensing Applications," 2019.
- [4] "Enhanced positive humidity sensitive behavior of p-reduced graphene oxide decorated with n-WS2 nanoparticles _Enhanced Reader.pdf." .
- [5] M. M. M. M. Mokhtar, S. H. Ismail, G. G. Mohamed, and M. Ibrahim, "Humidity Sensing Behaviour of Lyophilized rGO / Fe 2 O 3 Nanocomposite," no. April, 2020.
- [6] Z. Wu *et al.*, "Development of a rGO-BiVO 4 Heterojunction Humidity Sensor with Boosted Performance," 2021.
- [7] H. Dai, N. Feng, J. Li, J. Zhang, and W. Li, "Chemiresistive humidity sensor based on chitosan/zinc oxide/single-walled carbon nanotube composite film," *Sensors Actuators, B Chem.*, vol. 283, no. May 2018, pp. 786–792, 2019, doi: 10.1016/j.snb.2018.12.056.
- [8] M. T. S. Chani, K. S. Karimov, S. B. Khan, N. Fatima, and A. M. Asiri, "Impedimetric humidity and temperature sensing properties of chitosan-CuMn 2 O 4 spinel nanocomposite," *Ceram. Int.*, vol. 45, no. 8, pp. 10565–10571, 2019, doi: 10.1016/j.ceramint.2019.02.122.
- [9] Z. Chen *et al.*, "One-step fabrication of pyranine modified- reduced graphene oxide with ultrafast and ultrahigh humidity response," *Sci. Rep.*, vol. 7, no. 1, pp. 1–9, 2017, doi: 10.1038/s41598-017-02983-8.
- [10] E. Sensors and F. O. R. B. Applications, *Graphene-based electrochemical sensors for biomedical applications 12*. 2019.
- [11] Z. Duan *et al.*, "Daily writing carbon ink: Novel application on humidity sensor with wide detection range, low detection limit and high detection resolution," *Sensors Actuators, B Chem.*, vol. 339, no. April, p. 129884, 2021, doi: 10.1016/j.snb.2021.129884.
- [12] M. Tsai, P. Su, and C. Lu, "Sensors and Actuators : B . Chemical Fabrication of a highly sensitive flexible humidity sensor based on Pt / polythiophene / reduced graphene oxide ternary nanocomposite films using a simple one-pot method," vol. 324, no. August, 2020.
- [13] B. L. P. Eksperiandova and K. N. B. Pii, "Accepted Manuscript," 2016, doi: 10.1016/j.snb.2016.01.015.
- [14] S. G. Lee, J. Y. Seo, J. W. Lee, W. B. Park, K. S. Sohn, and M. Pyo, "Composition-tuned lithium aluminosilicate as a new humidity-sensing ceramic material with high sensitivity," *Sensors Actuators, B Chem.*, vol. 339, no. April, p. 129928, 2021, doi: 10.1016/j.snb.2021.129928.
- [15] H. Sensor, "Research Progress of Graphene-Based Flexible Humidity Sensor," 2020.
- [16] C. Lv *et al.*, "Recent Advances in Graphene-Based Humidity Sensors," *Nanomater. (Basel, Switzerland)*, vol. 9, no. 3, p. 422, Mar. 2019, doi: 10.3390/nano9030422.
- [17] A. G. Marrani, A. Motta, R. Schrebler, R. Zanoni, and E. A. Dalchiele, "Insights from experiment and theory into the electrochemical reduction mechanism of graphene oxide," *Electrochim. Acta*, vol. 304, pp. 231–238, May 2019, doi: 10.1016/J.ELECTACTA.2019.02.108.
- [18] M. Coros *et al.*, "Green synthesis, characterization and potential application of reduced graphene oxide," *Phys. E*, vol. 119, p. 113971, 2020, doi: 10.1016/j.physe.2020.113971.
- [19] N. Yadav and B. Lochab, "A comparative study of graphene oxide: Hummers, intermediate and improved method," 2019, doi: 10.1016/j.flatc.2019.02.001.
- [20] M. Saqib *et al.*, "High-Performance Humidity Sensor Based on the Graphene Flower/Zinc Oxide Composite," *Nanomater. (Basel, Switzerland)*, vol. 11, no. 1, p. 242, Jan. 2021, doi: 10.3390/nano11010242.
- [21] N. Sharma, M. Arif, S. Monga, M. Shkir, Y. K. Mishra, and A. Singh, "Investigation of bandgap alteration in graphene oxide with different reduction routes," 2020, doi: 10.1016/j.apsusc.2020.145396.
- [22] D. R. Kumar, S. Kesavan, M. L. Baynosa, V. Q. Nguyen, and J. J. Shim, "Flower-like Bi2S3 nanostructures grown on nitrogen-doped reduced graphene oxide for electrochemical determination of hydrogen peroxide," *J. Colloid Interface Sci.*, vol. 530, pp. 361–371, 2018, doi: 10.1016/j.jcis.2018.06.069.
- [23] K. Y. Rhee, "Electronic and Thermal Properties of Graphene," *Nanomater. (Basel, Switzerland)*, vol. 10, no. 5, p. 926, May 2020, doi: 10.3390/nano10050926.
- [24] C. Aksoy and D. Anakli, "Synthesis of Graphene Oxide Through Ultrasonic Assisted Electrochemical Exfoliation," *Open Chem.*, vol. 17, no. 1, pp. 581–586, 2019, doi: 10.1515/chem-2019-0062.
- [25] M. J. Deka and D. Chowdhury, "Surface charge induced tuning of electrical properties of CVD assisted graphene and functionalized graphene sheets," *J. Mater. Sci. Technol.*, vol. 35, no. 1, pp. 151–158, Jan. 2019, doi: 10.1016/j.jmst.2018.09.017.
- [26] A. Poniatowska, M. Trzaskowski, and T. Ciach, "Production and properties of top-down and bottom-up graphene oxide," 2018, doi: 10.1016/j.colsurfa.2018.10.049.

- [27] A. T. Smith, A. M. Lachance, S. Zeng, B. Liu, and L. Sun, "Synthesis, properties, and applications of graphene oxide/reduced graphene oxide and their nanocomposites," 2019, doi: 10.1016/j.nanoms.2019.02.004.
- [28] J. H. Lee, S. J. Park, and J. W. Choi, "Electrical property of graphene and its application to electrochemical biosensing," *Nanomaterials*, vol. 9, no. 2, 2019, doi: 10.3390/nano9020297.
- [29] L. Zhang *et al.*, "Wirelessly powered multi-functional wearable humidity sensor based on RGO-WS2 heterojunctions," *Sensors Actuators, B Chem.*, vol. 329, no. October 2020, 2021, doi: 10.1016/j.snb.2020.129077.
- [30] J. Fan, S. Zhang, F. Li, Y. Yang, and M. Du, "Recent advances in cellulose-based membranes for their sensing applications," *Cellul. (London, England)*, pp. 1–23, Sep. 2020, doi: 10.1007/s10570-020-03445-7.
- [31] S. Rahpeima *et al.*, "Reduced graphene oxide-silicon interface involving direct Si-O bonding as a conductive and mechanical stable ohmic contact," *Chem. Commun.*, vol. 56, no. 46, pp. 6209–6212, 2020, doi: 10.1039/d0cc02310h.
- [32] M. Sağlam, B. Güzeldir, A. Türüt, and D. Ekinçi, "Role of Reduced Graphene Oxide-Gold Nanoparticle Composites on Au/Au-RGO/p-Si/Al Structure Depending on Sample Temperature," *J. Electron. Mater.*, vol. 50, no. 8, pp. 4752–4761, 2021, doi: 10.1007/s11664-021-09017-0.
- [33] F. Ejehi, R. Mohammadpour, E. Asadian, P. Sasanpour, S. Fardindoost, and O. Akhavan, "Graphene Oxide Papers in Nanogenerators for Self-Powered Humidity Sensing by Finger Tapping," *Sci. Rep.*, vol. 10, no. 1, p. 7312, Apr. 2020, doi: 10.1038/s41598-020-64490-7.
- [34] R. Adib, Y. Lee, V. V Kondalkar, S. Kim, and K. Lee, "A Highly Sensitive and Stable rGO:MoS₂ - Based Chemiresistive Humidity Sensor Directly Insertable to Transformer Insulating Oil Analyzed by Customized Electronic Sensor Interface," 2021.
- [35] Q. Crystal *et al.*, "Reduced Graphene Oxide-Polyethylene Oxide Composite Films for Humidity Sensing via Quartz Crystal Microbalance," 2017.
- [36] D. Zhang, J. Tong, and B. Xia, "Sensors and Actuators B : Chemical Humidity-sensing properties of chemically reduced graphene oxide / polymer nanocomposite film sensor based on layer-by-layer nano self-assembly," vol. 197, pp. 66–72, 2014.
- [37] G. Hassan, M. Sajid, and C. Choi, "Highly Sensitive and Full Range Detectable Humidity Sensor using PEDOT : PSS , Methyl Red and Graphene Oxide Materials," pp. 1–10, 2019.
- [38] X. Guan *et al.*, "A flexible humidity sensor based on self-supported polymer film," *Sensors and Actuators B: Chemical*, vol. 358, 2022, doi: 10.1016/j.snb.2022.131438.
- [39] G. Naik and S. Krishnaswamy, "Room-Temperature Humidity Sensing Using Graphene Oxide Thin Films," *Graphene*, vol. 05, no. 01, pp. 1–13, 2016, doi: 10.4236/graphene.2016.51001.
- [40] M. Shojaee, S. Nasresfahani, M. K. Dordane, and M. H. Sheikhi, "Fully integrated wearable humidity sensor based on hydrothermally synthesized partially reduced graphene oxide," *Sensors Actuators, A Phys.*, vol. 279, pp. 448–456, 2018, doi: 10.1016/j.sna.2018.06.052.
- [41] T. Q. Trung, L. T. Duy, S. Ramasundaram, and N.-E. Lee, "Transparent, stretchable, and rapid-response humidity sensor for body-attachable wearable electronics," *Nano Res.*, vol. 10, no. 6, pp. 2021–2033, 2017, doi: 10.1007/s12274-016-1389-y.
- [42] R. Ranjan, M. Kumar, and A. S. K. Sinha, "CdS supported on electrochemically reduced rGO for photo reduction of water to hydrogen," *Int. J. Hydrogen Energy*, vol. 44, no. 21, pp. 10573–10584, Apr. 2019, doi: 10.1016/j.ijhydene.2019.02.195.
- [43] G. Zhao and G. Liu, "Electrochemical deposition of gold nanoparticles on reduced graphene oxide by fast scan cyclic voltammetry for the sensitive determination of As(III)," *Nanomaterials*, vol. 9, no. 1, 2019, doi: 10.3390/nano9010041.
- [44] D. P. Rocha *et al.*, "Chemically versus electrochemically reduced graphene oxide: Improved amperometric and voltammetric sensors of phenolic compounds on higher roughness surfaces," *Sensors Actuators B*, vol. 254, pp. 701–708, 2018, doi: 10.1016/j.snb.2017.07.070.
- [45] S. Siracusano, S. Trocino, N. Briguglio, V. Baglio, and A. S. Aricò, "Electrochemical impedance spectroscopy as a diagnostic tool in polymer electrolyte membrane electrolysis," *Materials (Basel)*, vol. 11, no. 8, 2018, doi: 10.3390/ma11081368.
- [46] Y. Huang, A. Hara, C. Terashima, A. Fujishima, and M. Takai, "Protein adsorption behavior on reduced graphene oxide and boron-doped diamond investigated by electrochemical impedance spectroscopy," *Carbon N. Y.*, vol. 152, pp. 354–362, Nov. 2019, doi: 10.1016/J.CARBON.2019.06.023.
- [47] T. Chandrakalavathi, K. R. Peta, and R. Jeyalakshmi, "Enhanced UV photoresponse with Au nanoparticles incorporated rGO/Si heterostructure," *Mater. Res. Express*, vol. 5, no. 2, p. 025011, Feb. 2018, doi: 10.1088/2053-1591/aaa9ac.

- [48] G. Darabdhara, M. R. Das, S. P. Singh, A. K. Rengan, S. Szunerits, and R. Boukherroub, "Historical perspective Ag and Au nanoparticles/reduced graphene oxide composite materials: Synthesis and application in diagnostics and therapeutics," 2019, doi: 10.1016/j.cis.2019.101991.
- [49] A. K. Das, J. E. Abraham, M. Pandey, and B. Manoj, "Impedance and electrochemical studies of rGO/Li-ion/PANI intercalated polymer electrolyte films for energy storage application," *Mater. Today Proc.*, vol. 24, pp. 2108–2114, 2019, doi: 10.1016/j.matpr.2020.03.667.